

Full Length Research Paper

GaN/SiC heterostructure field-effect transistor model including polarization effects

M. Rezaee Rokn-Abadi

Physics Department, Ferdowsi University of Mashhad, Mashhad, Iran. E-mail: roknebad@um.ac.ir.

Accepted 21 August, 2010

Self-consistent Monte Carlo simulation are reported for GaN/SiC HFETs. Hot carrier scattering rates are determined by fitting experimental ionisation coefficients and the doping character of GaN is obtained from substrate bias measurements. Preliminary simulations for a simple model of the GaN surface are described and results are found to be consistent with experimental data. Planer GaN/SiC HFETs structures with a 60 nm GaN pseudomorphically strained layer were simulated, where the spontaneous and piezoelectric polarization effects were taken into account. The polarization effects was shown to not only increase the current density, but also improve the electron transport in the interface layer by inducing a higher electron density to the positive polarized sheet and away from the buffer layer.

Key words: Monte Carlo simulation, piezoelectric, polarization effects, current density.

INTRODUCTION

GaN and SiC are currently of great interest both for short wavelength optoelectronics and for microwave power devices. The high breakdown field allows large voltage swings on the drain terminal of a FET and heat sinking through substrates allows very high power output. The saturated drift velocity for electrons is thought to be higher than 105 m/s. Though this is at a relatively high electric fields. High channel electron mobility is also available for HEMTs. Consequently it is possible to achieve good high frequency performance. The observed concentration of line defects in devices fabricated on GaN and SiC are still rather high ($>10^8 \text{ cm}^{-3}$) and trapping effects are also observed in the transport characteristics through current slump phenomena. It is therefore likely that defect related mechanisms may be masking the true potential of the material in current experimental observations.

In the present paper we develop a Monte Carlo model for GaN/SiC heterojunction field effect transistors (HFETs) which can sustain high current densities at elevated temperatures (Ando et al., 2000). Further contributing to the outstanding performance of GaN/SiC based HFETs is the ability to achieve two dimensional electron gases (2DEGs) with sheet carrier concentration up to 10^{13} cm^{-2} close to the interface, well in excess of those observed in other III-V material systems. This is

because of a lattice mismatch between GaN and its SiC buffer layer. In a typical GaN/SiC heterostructure an GaN layer is grown on top of a thick SiC layer. Because the lattice constant of SiC is larger than that of GaN, the GaN is grown pseudomorphically, with a biaxial tensile strain and a compressive strain along its hexagonal c-axis (Di and Brennan, 1991). This strain produces a macroscopic piezoelectric polarization field in the GaN/SiC interface. The direction of the field depends on the polarity of the GaN growth surface. Recent studies have indicated that in typical GaN/SiC, which are grown by metalorganic vapor phase epitaxy (MOVPE), this surface (which is [0001]) has cation polarity so that the orientation of the field is in the same direction as the growth (Liu et al. 2000).

DEVICE, MODEL AND SIMULATIONS

Figure 1 shows the structure of the simulated HFET which is based on the transistor studied experimentally and reported by Look et al. (Look et al., 1998). The device consists of a 78 nm top Al_{0.2}Ga_{0.8}N layer with doping density of $5 \times 10^{23} \text{ m}^{-3}$. An electron concentration of $3 \times 10^{24} \text{ m}^{-3}$ is assumed for the source and drain contact regions. The overall device length is 3.5 μm in the x-direction and the device has a 0.45 μm gate length and 0.5 μm source and drain length. The top and down buffer layers are dropped

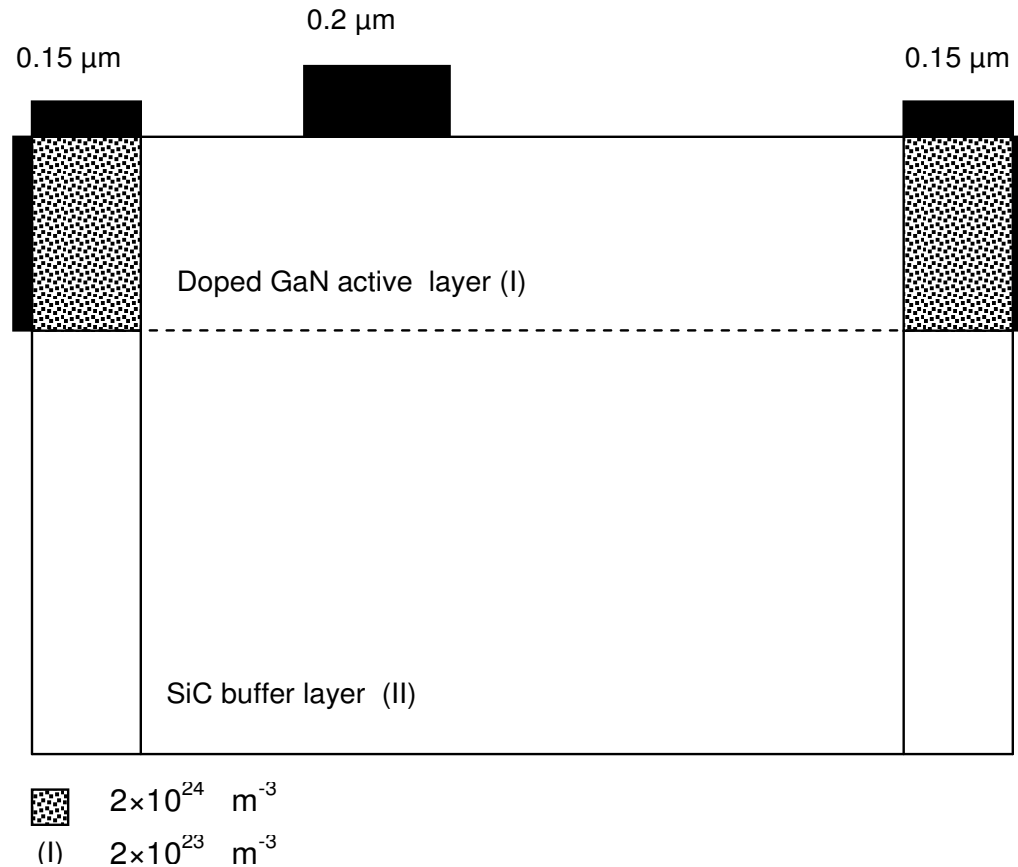


Figure 1. Cross section of the $\text{Al}_{0.2}\text{Ga}_{0.8}\text{N}/\text{GaN}$ structures which have chosen in the simulation.

to 10^{23} and 10^{22} m^{-3} , respectively. The effective source to gate and gate to drain separation are 0.8 and $1.25 \mu\text{m}$, respectively. A Schottky barrier height of 1 eV for the gate electrode has been used to represent the contact potential at the Au/Pt. The source and drain have ohmic contacts which are modelled with the geometry shown in Figure 1. The side contacts are intended to represent the remainder of the ohmic pads in the real device.

The ensemble Monte Carlo method used as the basis for this work was developed in Durham university and has been used extensively in the study of the electronic properties of many semiconductors and device structures including AlGaInP/GaAs HBTs, InGaAs/InP HEMTs and InGaAsP quantum well lasers (Makino et al., 2001).

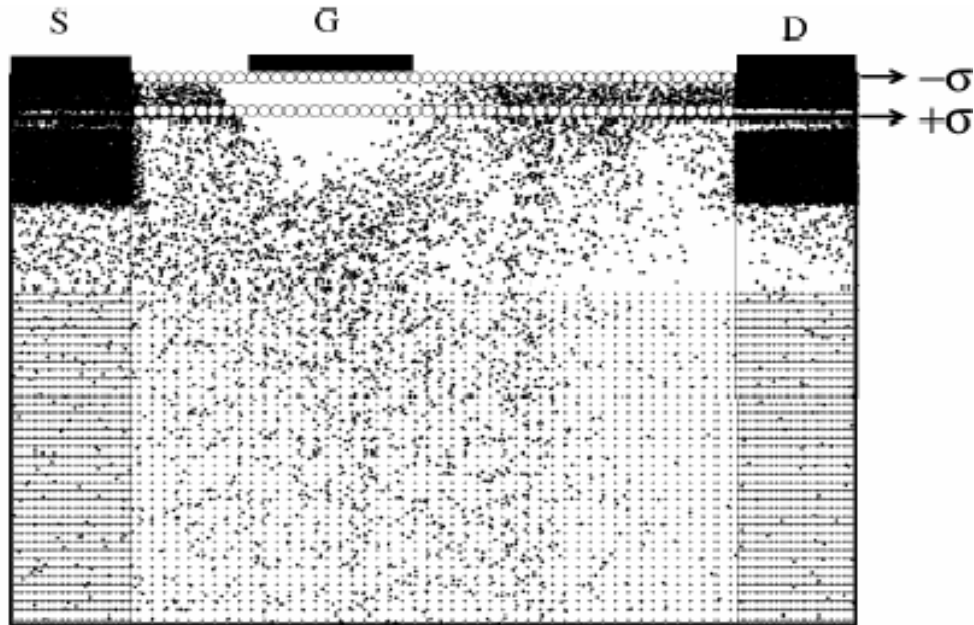
In the case of the ellipsoidal, non-parabolic conduction valley model, the usual Herring-Vogt transformation matrices are used to map carrier momenta into spherical valleys when particles are drifted or scattered. The Monte Carlo simulation includes impurity scattering and all of the standard phonon scattering processes (Ridley, 1997). It also allows for alloy scattering and piezoelectric scattering. The familiar five-valley approximation of the first two conduction bands has been used for the wurtzite crystal structure of GaN. In order to minimize the statistical fluctuations, always associated with the stochastic Monte Carlo method, we choose 20000 electrons with a Dirichlet boundary conditions for each mesh point. The timestep between two updates of the electric field is taken to be 1 fs .

Figure 2 illustrates the instantaneous distribution of 20000 electron particles at steady-state forward bias (drain voltage 30 V and gate voltage -1 V) superimposed on the field cell mesh in the

simulated HFET structure (Jacoboni et al., 1989). In order to represent the polarization across the heterostructure interface, fixed superparticles (charge per unit length) are placed in the upper and lower of that layer as shown in Figure 2, with the positive charge at the interface layer (Moglestue, 1993). In the simulation presented here it is assumed that polarization charges are of density $2 \times 10^{13} \text{ cm}^{-2}$ to take into account the spontaneous and piezoelectric polarization effects (Mansour et al., 1991). However, the positive polarization charge at the AlGaIn/GaN interface tends to be compensated by the free electrons which are attracted to it. Because of the buffer layer's important role in high-field trapping effects, it is assumed in the simulations that trap centres are in buffer layer with density of 10^{23} m^{-3} , capture cross-section of $2 \times 10^{-19} \text{ m}^2$ and energy of 0.3 eV . This trap centres are fixed at the centre of each electric field cell and captured some mobile charges.

RESULTS

To study the polarization effect on device performance, we have simulated the GaN HFET shown in Figure 1 with and without the inclusion of the polarization effect. The simulation results indicate that the steady-state drift velocity and electronic transport properties of the device increase with the inclusion of the polarization effect across the interface which is in good agreement with the recent theoretical work done by Ando et al., (2000)



- Mobile electrons
- Fixed polarisation particles
- Fixed electron traps

Figure 2. Particles in the Monte Carlo simulation of $\text{Al}_{0.2}\text{Ga}_{0.8}\text{N}/\text{GaN}$ HFET are of two types. These are fixed particles which represent the polarization charges and trap centres and the mobile superparticles which represent unbound electrons which can flow through the device.

who were used two dimensional self-consistent full band Monte Carlo simulation for $\text{Al}_{0.2}\text{Ga}_{0.8}\text{N}/\text{GaN}$ HFETs including piezoelectric polarization effects. The main reason for this can be understand from the simulated I-V characteristic for the polarization and the polarization-free device, it can be observed that polarization leads to an enhancement of the drain saturation current from 1250 mA mm^{-1} to 1650 mA mm^{-1} at zero gate bias. This pattern of output current enhancement is due to the use of a heterostructure and the fact that the polarization charge encourages a higher electron density at the heterointerface where trapping does not occur and the electron mobility is high. The associated intrinsic transconductance derived from the current-voltage characteristics at knee voltage ($\sim 18 \text{ V}$) for the simulated device without polarization charge and with including polarization charge are 85 and 110 mS mm^{-1} , respectively.

Figure 3 compares the electron density recorded from the buffer to the gate for both polarization and polarization-free devices. It can be seen that for the same bias condition the electron density in the interface region is increased for polarization device. This results an increase in electric field transverse to the channel and cause an enhancement in output drain current.

Furthermore, high electric field in the gate and interface region can sustain high velocities in these regions. We can estimate the speed of the device from the average electron transit time along the channel. By summary the transit times for each field cell we estimate the transit time to be $\tau = 2.6 \text{ ps}$. Hence the intrinsic cut-off frequency is about $f_t = 1/2\pi\tau \approx 60 \text{ GHz}$. Figures 4a and b show a contour plot of the conduction band edge for the polarization and polarization-free devices, respectively. The source is located on the left and the drain is on the right. It is noticeable that much of the drain-source bias in the polarization-free device is dropped in the vicinity of the gate region. The sharp drop in potential at the drain edge of the gate generates hot electrons which can diffuse into the AlGaN layer and also into the GaN buffer layer where they can be trapped.

In comparison Figure 4b shows results for polarization charge density of $2 \times 10^{13} \text{ m}^{-2}$. It is seen that the presence of polarization charge reduces the sharp potential drop seen in Figure 4a as a result of the high electron density around the heterointerface, and also strongly affects the potential between source and gate. This improves electron confinement, which is the main reason for a higher output drain current.

To study the effect of the magnitude of the polarization

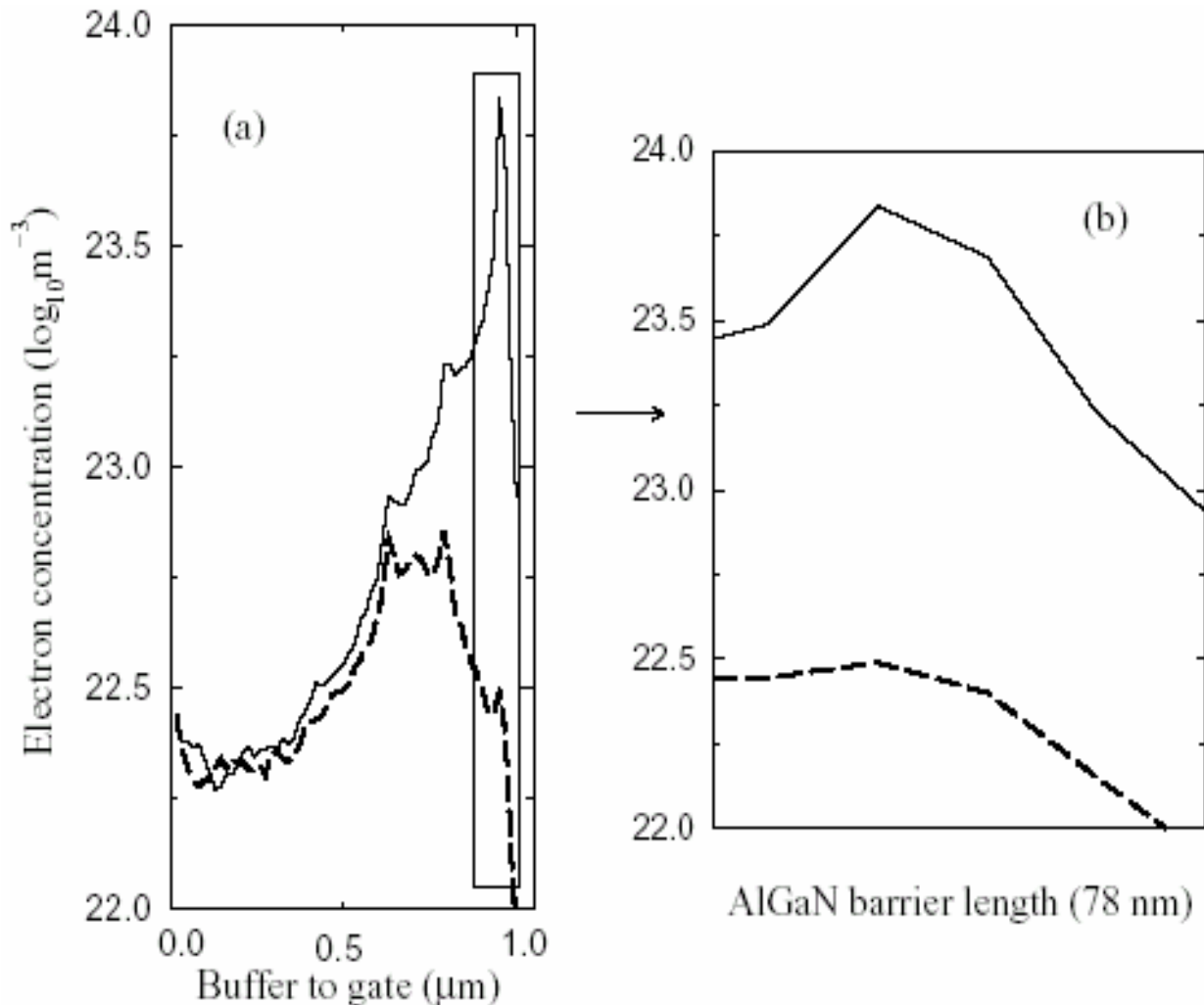


Figure 3. Electron density through the device under the gate extracted along the vertical line from the buffer to the centre of gate.

charge density on electronic transport in more detail, Monte Carlo simulations of steady-state condition were performed for a range of different densities. Figure 5a and b compare semiquantitatively the electron distribution around the heterointerface for two different charge densities. It can be seen that with increasing polarization charge density the number of electrons occupying the channel region increases. It can be calculated that the electron drift velocity increases from 1.9×10^5 to 2.7×10^5 ms^{-1} as σ goes from 10^{12} to 2×10^{13} m^{-2} due to an increased electric field transverse to the channel.

Summary

In this article, we have presented the results of a Monte Carlo simulation for electron transport in Al_{0.2}Ga_{0.8}N/GaN HFETs which was developed to show the spontaneous and piezoelectric polarization effects.

Using valley model to describe the electronic bandstructure, calculated drain currents was shows the polarization effect not only increase the output current, but also improve the electron transport in the interface layer by inducing a higher electron density to the positive sheet and hence it can improve transconductance. The presented results are in fair agreement with other calculation.

However, the simulation results can provide some guide to the range within which AlGa_N/Ga_N HFET with a specific polarization charge is expected to have the better performance.

ACKNOWLEDGMENTS

This work is supported by the Ferdowsi University of Mashhad through a contract with Vive president for Research and Technology.

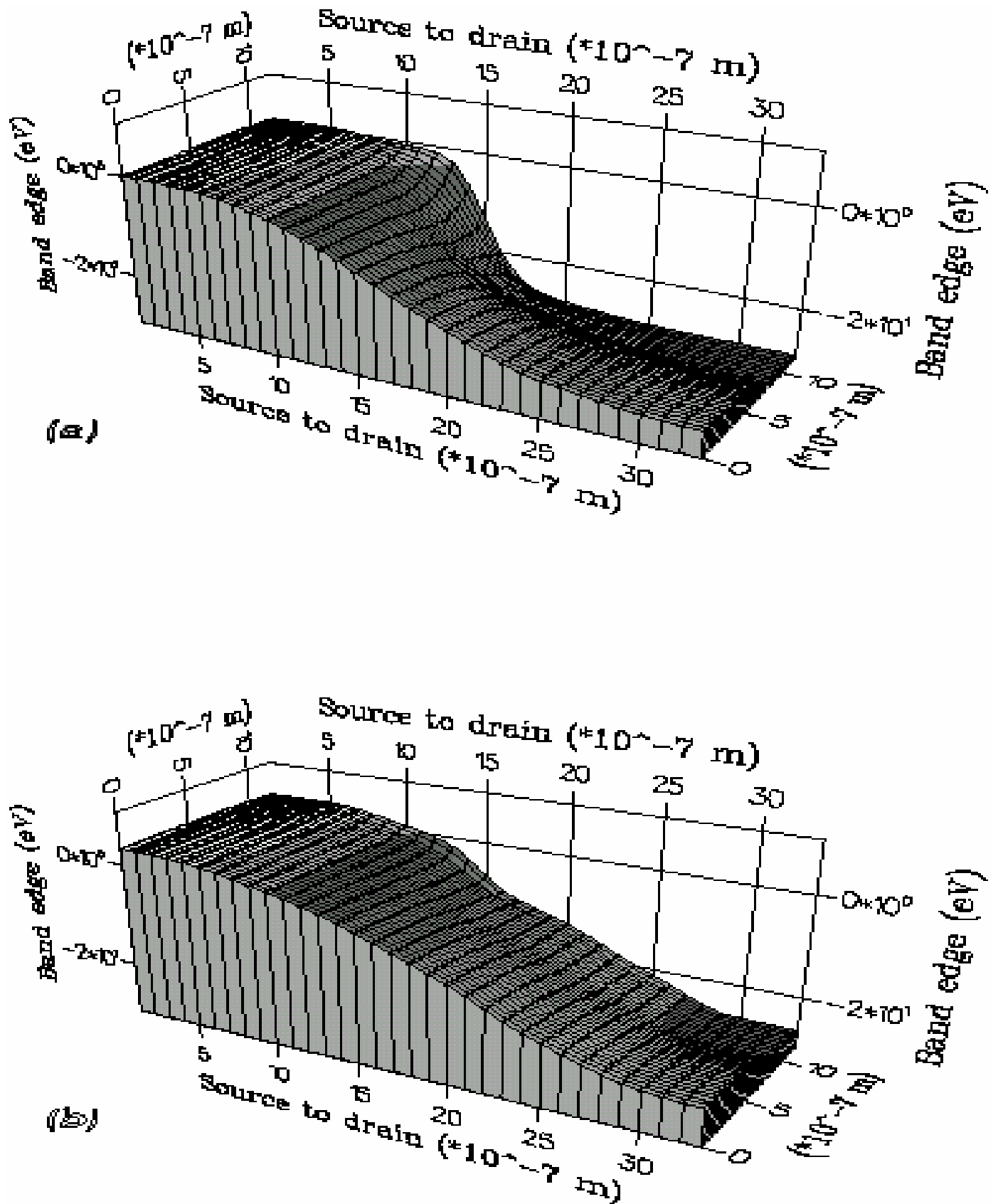


Figure 4. Three-dimensional distribution of the conduction band profile in the simulated GaN HFET at room temperature. (a) without polarization charge at the interface layer and (b) with polarization charge density.

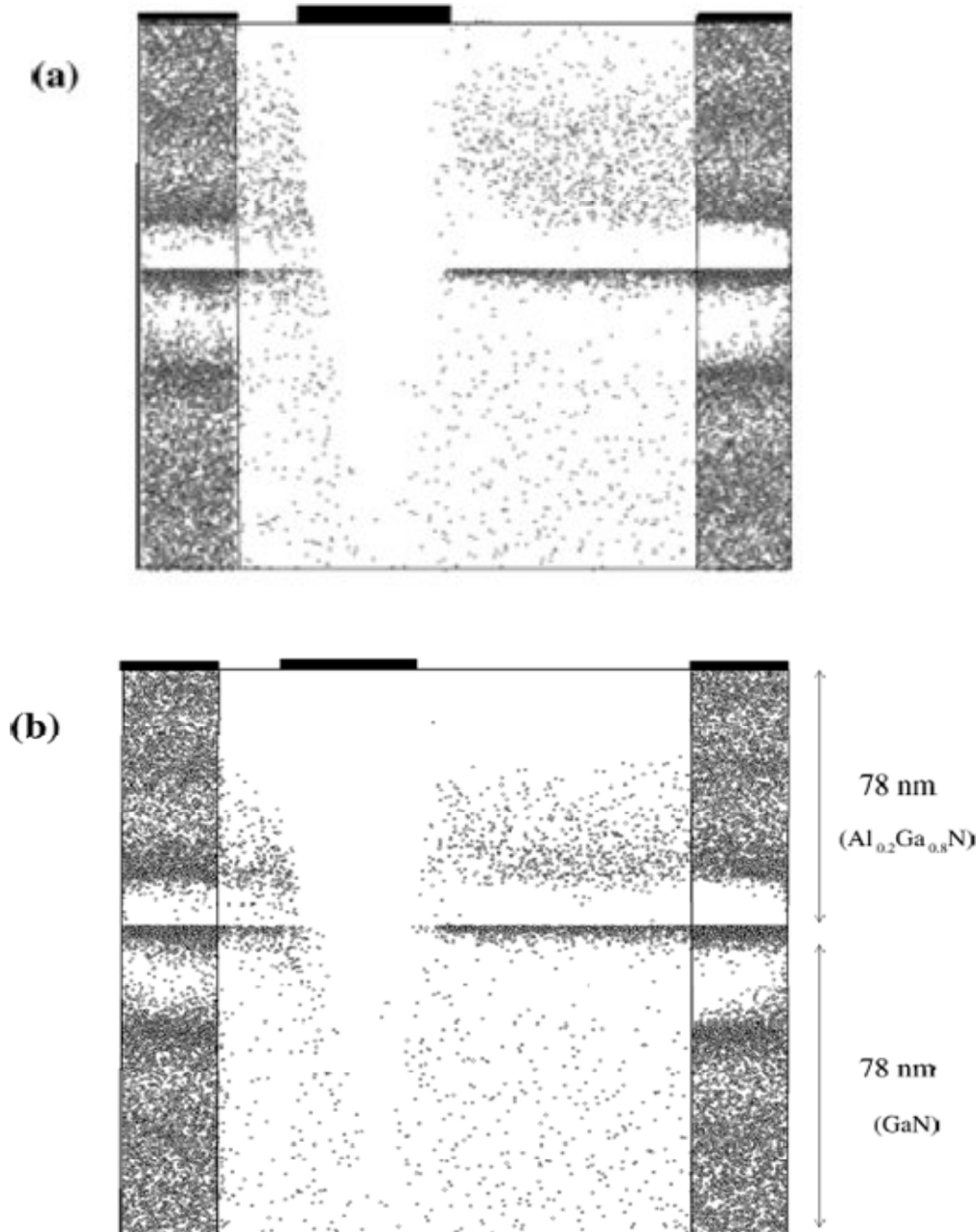


Figure 5. Effect of different polarization sheet charge densities on electron distribution through the wurtzite GaN HFET at room temperature when $V_{gs} = -1$ V and $V_{ds} = 30$ V. (a) $\sigma = 10^{12}$ cm $^{-2}$ and (b) $\sigma = 2 \times 10^{13}$ cm $^{-2}$.

REFERENCES

- Ando Y, Contrata W, Samoto N, Miyamoto H, Matsunaga K, Kuzuhara M (2000). IEEE Transactions on Electron Devices, 47: 1965.
- Di K, Brennan K (1991). Comparison of electron transport properties in ZnS and ZnSe. J. Appl. Phys., 69: 3097
- Jacoboni C, Lugli P (1989). The Monte Carlo Method for semiconductor and Device Simulation, Springer-Verlag.
- Liu Y, Gorla CR, Liang S, Emanetoglu N, Wraback M (2000). Crystal growth in ZnS. J. Electron. Mater., 29: 69.
- Look DC, Reynolds DC, Sizelove JR, Harsch WC (1998). Effect of plasmon scattering in semiconductor devices. Solid Stat. Commun., 105: 399.
- Makino T, Segawa Y, Ohtomo A (2001). Electron mobility in high electric field application. Appl. Phys. Lett., 78: 1237.
- Mansour N, Di K, Brennan K (1991). Full band Monte Carlo simulation in GaN material. J. Appl. Phys., 70: 6854.
- Moglestue C (1993). Monte Carlo Simulation of Semiconductor Devices, Chapman and Hall.
- Ridley BK (1997). Electrons and phonons in semiconductor multilayers, Cambridge University Press.